Supporting Informations

Unidirectional photoisomerization of styrylpyridine for switching the magnetic behavior of an iron(II) complex: a MLCT pathway in crystalline solids.

Antoine Tissot, † Marie-Laure Boillot, † Sébastien Pillet, ‡ Epiphane Codjovi,§ Kamel Boukheddaden,§ Latévi Max Lawson Daku #*

† ICMMO, ECI, UMR CNRS 8182, Université Paris-Sud 11, 15 Rue Georges Clémenceau, 91 405 Orsay, France.

‡ CRM2, UMR CNRS 7036, Institut Jean Barriol, Nancy-Université, BP239, 54506 Vandoeuvre les Nancy, France.

§ GEMAC, UMR 8635, Université de Versailles-Saint Quentin en Yvelines, 45 Avenue des Etats-Unis, 78035 Versailles cedex, France.

Faculté des Sciences, Université de Genève, 30 Quai Ernest-Ansermet, CH-1211 Genève, Switzerland.

Optical investigation:

A calculated value of the refractive index is obtained from the experimental extinction coefficient spectra using the KK relations and compared to the experimental one. The results corresponding to an irradiation time of 60 min (of the all-cis compound) are depicted in Figure S1. They show clearly that KK relations are well verified, although a small deviation is observed in the UV region, attributed to the presence of the cutoff in the spectra at 246 nm, which renders the KK relation hardly applicable.

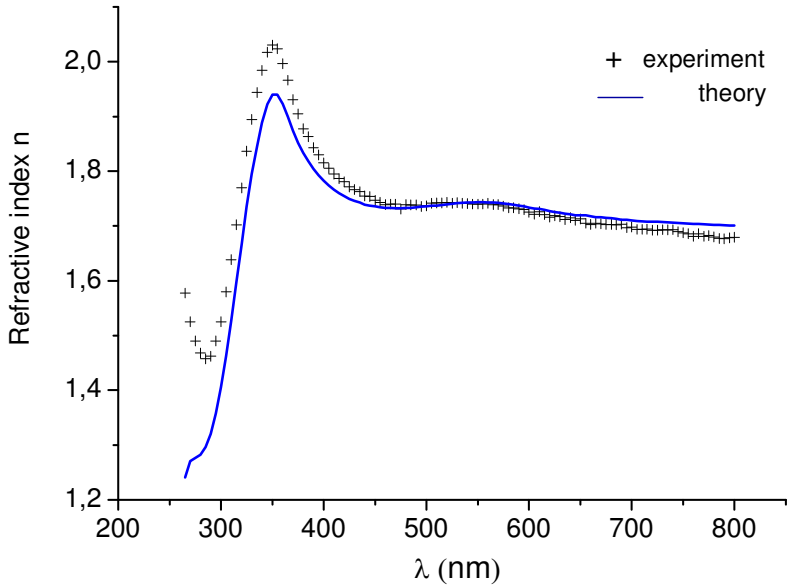

Fig. S1: Comparison between the experimental refractive index spectrum and the calculated one using Kramers-Kronig relations.

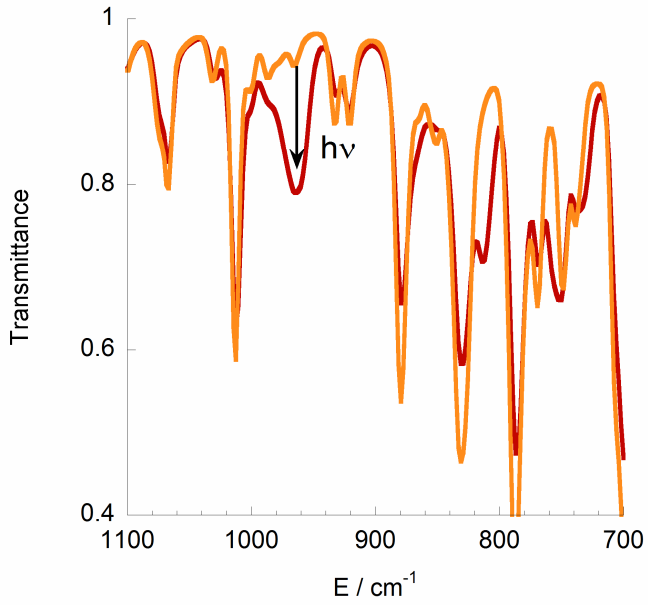

Fig S2: RT ATR-IR characterizations of the all-cis species (in the form of a pellet) and its evolution during the UV excitation (λ = 365 nm).

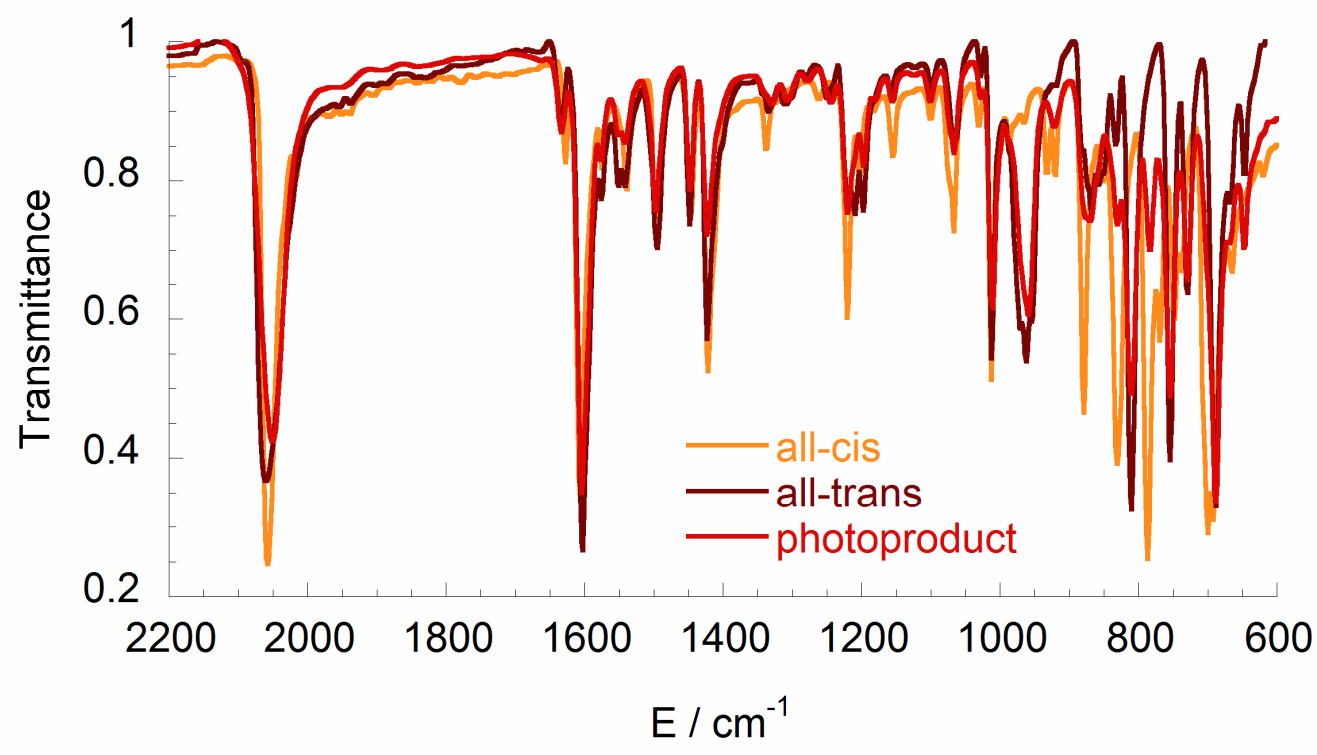

Fig S3: RT ATR-IR spectra of all-cis, all-trans and photogenerated (λ_{exc} = 532 nm) compounds.

X-Ray Diffraction investigation:

The crystal structure of the photo-perturbed crystalline phase has been derived from X-ray diffraction measurements by stopping the illumination before the complete amorphization of the material. The corresponding crystal structure may be rather seen as an indication of the transformation process, and may not be confused with the crystal structure of the real photo-product as usually reported in similar photocrystallographic studies. From this data, there is no way to estimate the photoconversion yield of this state. Crystal data and refinement details are given in Table S1. It is to be noted that, owing to the almost complete amorphization at t = 50 min, the measured diffraction data were of limited quality; only the data up to θ_{max} = 25.35° proved to be quite significant and were included in the structural refinement. For purpose of comparison, a similar cut-off was used for the structural refinement of the parent all-cis structure. The structure was solved by direct methods and refined on F^2 using SHELXL97. Non-hydrogen atoms were refined anisotropically, hydrogen atoms were generated at their ideal positions.

Table S1: Crystal data and structure refinement details for $Fe(stpy)_4(NCSe)_2$.

	Parent all-cis	Photo-perturbed crystalline phase (50 min excited)
Empirical formula	$C_{54}H_{44}N_6Se_2Fe$	
fw / g.mol^{-1}	990.72	
T/K	293(2)	293(2)
Crystal System	Monoclinic	Monoclinic
Space group	C2/c	C2/c
a / Å	19.748(1)	19.8351(8)
b / Å	13.253(1)	13.2297(5)
c / Å	18.335(1)	18.4588(8)

β / °	95.081(5)	94.398(4)
V / Å^3	4779.8	4829.5(4)
Z	4	4
ρ_{calc} / g cm^{-3}	1.38	1.38
μ / mm^{-1}	1.88	1.88
Measured data	16502	29606
θ_{max}	25.35	25.35
R_{int} [a]	0.047	0.062
Independant data	4380	4419
wR2 [$F^2 > 2\sigma(F^2)$] [b]	0.109	0.132
R1 [$F^2 > 2\sigma(F^2)$] [c]	0.047	0.059

[a] $R_{\text{int}} = \sum (N/N-1) \sum_i |I_i - \langle I \rangle| \Big/ \sum \sum_i I_i$. [b] $wR2 : \left(\sum \left[w \left(F_o^2 - F_c^2 \right)^2 \right] \Big/ \sum \left[w \left(F_o^2 \right)^2 \right] \right)^{1/2}$. [c] $R1 : \sum \| F_o | - F_c | \Big/ \sum |F_o|$.

Table S2: Relevant structural parameters

	Parent all-cis	Photo-perturbed crystalline phase
Fe-N1 (Å)	2.143(3)	2.124(4)
Fe-N2 (Å)	2.226(3)	2.233(4)
Fe-N3 (Å)	2.234(3)	2.234(3)
<Fe-N>	2.201	2.197
Σ (°)[a]	36.2	32.1

[a] Σ is defined as the sum of the absolute values of the deviation from 90° of the 12 cis angles in the coordination sphere.

Table S3: Intermolecular distances shorter than the sum of the Van der Waals radii at 293 and 104 K for Fe(trans-stpy)$_4$(NCSe)$_2$ and Fe(cis-stpy)$_4$(NCSe)$_2$. The labelling of atoms is shown in *Inorg. Chem.* **2009**, *48*, 4729.

	all-trans 104 K	all-trans 293 K
Se3 • • • C42	3.544(2)	3.593(5)
Se2 • • • C15	3.829(3)	3.907(5)
Se2 • • • C26	3.845(3)	3.925(8)
C7 • • • C27	3.614(3)	3.719(7)
C7 • • • C28	3.419(3)	3.517(6)

	all-cis 104 K	all-cis 293 K
C19 • • • C14	3.387(3)	3.501(5)
C21 • • • C7	3.298(3)	3.365(5)
C16 • • • C8	3.681(3)	3.757(5)
C16 • • • C9	3.578(3)	3.622(5)
C16 • • • C14	3.518(4)	3.560(5)

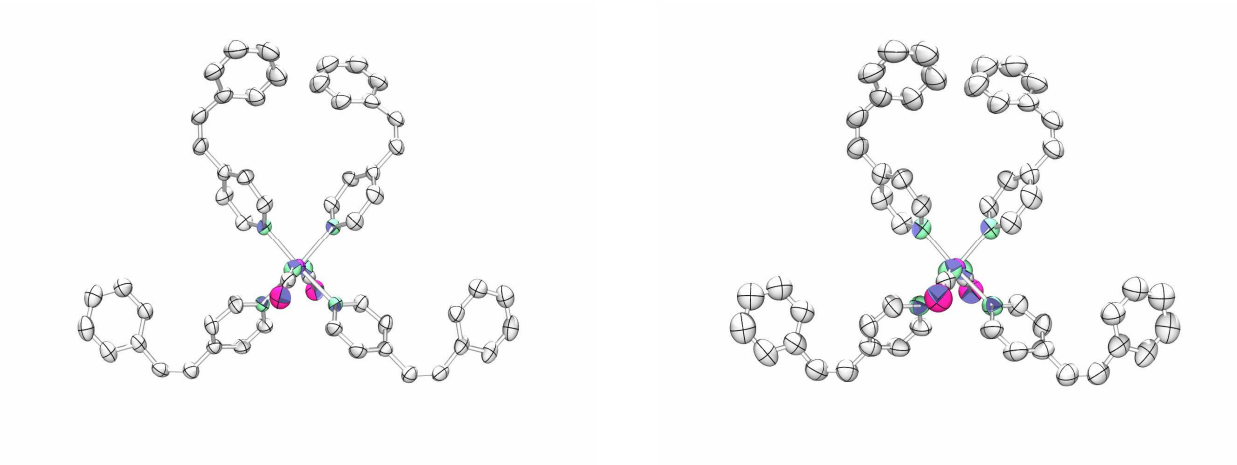

Fig. S4. ORTEP drawing with 50% probability ellipsoids of the all-cis reactant structure (left) and the photo-perturbed crystalline phase (right).

The obtained crystal structure of the photo-perturbed crystalline phase is very close to the reference all-cis parent structure previously reported at room temperature (Table S1). The mean atomic position deviation (root mean square deviation) between the two molecular structures is only 0.04 Å. Besides the slight change in unit cell parameters, we do not observe any space group change (C2/c). The most relevant structural parameters are listed in Table S2, together with those previously reported for all-cis.

We do not observe any change of conformation of the stpy ligands, which would have been expected for a cis to trans photo-induced isomerization. The most prominent structural modification is a 0.02 Å shortening of the Fe-N1 coordination distance. On the contrary, the mean Fe-N coordination distance is left almost unchanged. Owing to the uniform unit-cell expansion, the intermolecular Fe…Fe distances increase significantly.

The comparison of the molecular structures of all-cis reactant and photo-perturbed crystalline phase shows significant modifications of the vibrational ellipsoids (Figure S4); it is obvious that the atomic displacement parameters are significantly higher in the photo-perturbed crystalline structure, than in the reactant structure. We consider that this trend is not the result of higher vibration amplitudes, but rather a consequence of a larger distribution in atomic positions for the former. This assertion is in line with the progressive amorphization of

the sample. According to all these observations, we can indeed conclude that the crystal structure we derive here is not the crystal structure of the real photoconverted material, but rather the structural signature of the residual all-cis reactant molecules, which are still not photoconverted yet. (see the schematic diagram in figure 4b). Unfortunately, our diffraction data does not afford the possibility to observe the structure of the photoconverted molecules, whether they result from a putative all-cis to all-trans photoisomerization or even a partial cis-to-trans isomerization involving only part of the stpy ligands.

Reflectivity measurements:

The powder samples was thermally cycled at least ten times between the liquid nitrogen and room temperature, before starting the measurements between 270 and 80 K. The repeated application of such thermal shocks led to auto-milling of the sample into smaller crystals, which is thought to release internal stresses due to grain boundaries and definitely improves the reproducibility of the data.

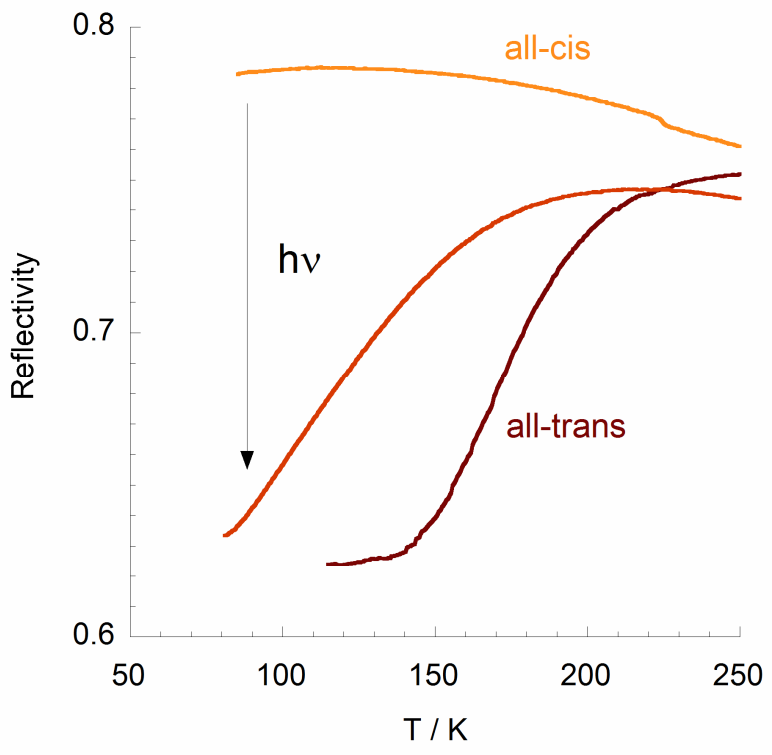

Fig S5: VT diffuse reflectivity data recorded for all-cis, all-trans and photogenerated (λ_{exc} = 532 nm) compounds.

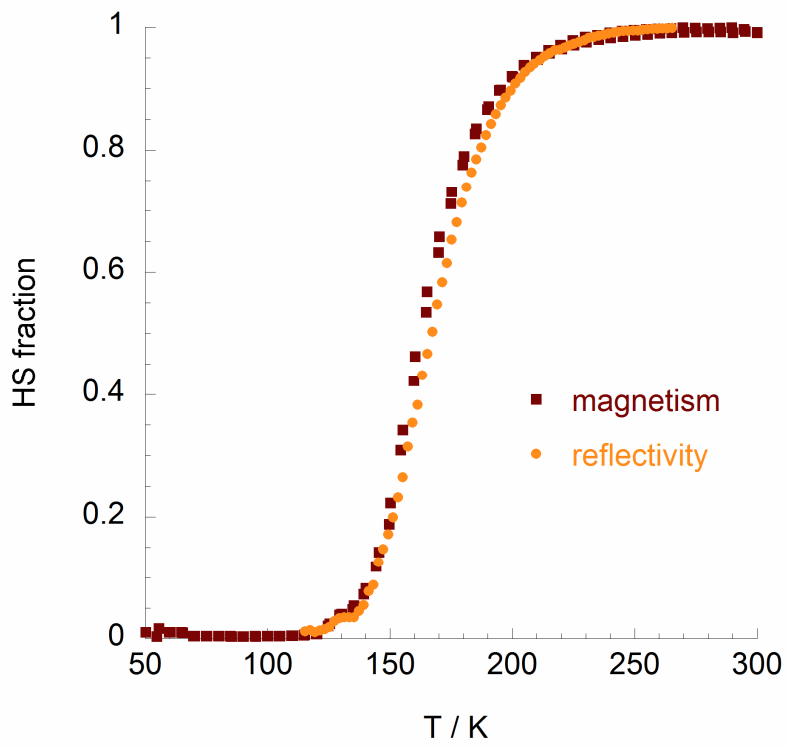

Fig S6: Temperature dependence of the HS fraction determined for the all-trans compound: from diffuse reflectivity measurements via a Kubelka-Munck treatment and magnetic measurements.

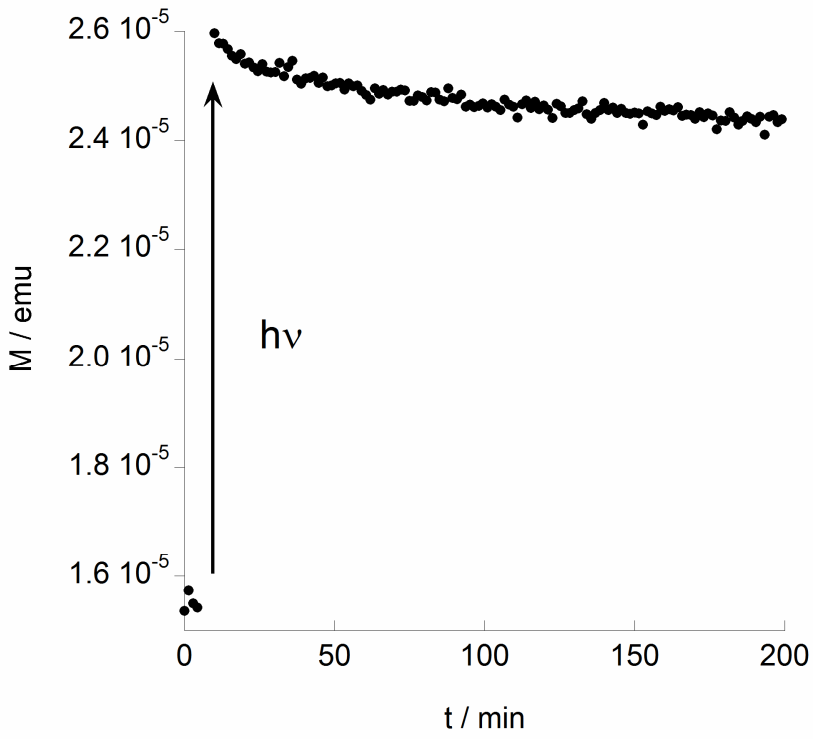

Fig S7: LIESST effect probed at 10 K by magnetization measurement. The *in-situ* photo-excitation of the photoproduct was carried out with $\lambda = 532$ nm.